ACS Energy LETTERS

http://pubs.acs.org/journal/aelccp

VIEWPOINT

A Guide to Electrocatalyst Stability Using Lab-Scale Alkaline Water Electrolyzers

Cite This: *ACS Energy Lett.* 2024, 9, 547−555

Read Online

ACCESS | Metrics & More | Article Recommendations | Supporting Information

Hydrogen is expected to play a critical role in the electrification and decarbonization of industrial and commercial sectors, becoming increasingly cost-competitive with large-scale fossil fuels.[1−3] Green hydrogen from low-temperature water electrolysis has received significant attention with a projected thousand-fold global capacity expansion by 2030.[4] This technology branches into three configurations: proton exchange membrane (PEM) electrolysis, alkaline water electrolysis (AWE), and anion exchange membrane (AEM) electrolysis.[5] Despite differences in components and operating conditions, all these configurations share common challenges, necessitating systematic optimization for large-scale industrialization.[6]

Electrocatalysis is critical in water electrolysis research and a prominent topic in *ACS Energy Letters*.[7] However, despite a surge in publications claiming "outstanding" or "excellent" electrocatalytic activity, very few attempts have been made to examine their performance in more realistic setups. This trend has led to an increase in publications that fail to advance the scientific or engineering knowledge of critical challenges in water electrolysis.[8] These publications come out partly due to inadequate testing environments and operating conditions. Contrary to PEM and AEM electrolysis research, where catalysts have been integrated into the more realistic membrane-electrode assembly (MEA), AWE academic research primarily uses three-electrode cell configurations, poorly representative of practical electrolyzers.[1,9−11] Testing conditions and stability limits differ significantly when comparing electrocatalysts in laboratory and industrial settings.[5,9,12−14] Thus, there is an urgent need for testing under realistic settings to capture compounded instability from all components, not just the catalyst.[1]

Electrochemical flow cells provide a reliable platform for transitioning to more realistic settings by imitating MEA-like conditions and facilitating device-level evaluation of electrocatalysts.[1,10,15] Flow cells enable testing full cell configurations, where component interactions can affect overall performance or introduce new stresses.[16,17] Moreover, flow cells can be a powerful tool for examining the durability of electrocatalysts at the lab scale.[18] Beyond only reporting the catalytic activity, there is an urgent need in the AWE field to understand practical issues, including catalyst deactivation, gas crossover, and bubble removal.[19,20] These aspects are critical under high current density conditions, as the operating environment is drastically different from laboratory configurations where local pH changes, corrosion, and mass transfer are typically neglected.[18] Understanding electrocatalyst integration into flow cells and their response to industrially relevant conditions is crucial for advancing commercially viable technologies.[2,12]

A substantial challenge in AWE research is the lack of standardized protocols. Unlike PEM electrolysis and fuel cell research,[10,11,21−23] the AWE community still lacks standardized procedures for cell configurations, device assembly, accelerated stress tests, reference materials, and reporting data. Despite noteworthy efforts,[5,24,25] the scarcity of standardized lab-scale alkaline electrolyzer protocols impedes precise comparisons and reproducibility, leading to several groups creating custom architectures and employing unique testing conditions.[26] Establishing methods for accurate electrocatalyst comparison across laboratories is therefore imperative.[12,27]

To advance electrocatalysis research in the AWE community, we report a standardized electrochemical flow cell setup, refined after four years of development and optimization by our group. This Viewpoint outlines the operation of this device in a laboratory setting, primarily for studying electrocatalytic stability. Our design aims for simplicity and affordability, making it suitable for researchers attempting to examine stability in more realistic settings immediately after the initial screening of promising catalysts using three-electrode cells. In the scaling-up pathway for AWE, our approach would logically follow three-electrode cell testing and precede more sophisticated electrolyzer setups mimicking industrial operation.[5,26]

To facilitate the reproducibility of our approach across the AWE community, the Supporting Information includes a comprehensive guide on electrolyzer manufacture, assembly, integration, operation, and troubleshooting. Furthermore, we describe three case studies demonstrating the electrolyzer performance: a Ni electrode, a benchmark NiFe anode for the oxygen evolution reaction (OER), and a nickel nitride (Ni_3N) precatalyst. We also propose standard protocols for testing electrocatalytic stability under fluctuating and reverse currents.

This work, inspired by similar advances in CO_2 electrolysis,[28] represents the next step in AWE electrocatalysis

Received: December 20, 2023
Accepted: January 17, 2024
Published: January 23, 2024

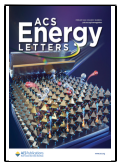

research. As illustrated in Figure 1, lab-scale electrochemical flow cells harmonize stability evaluation and mark an

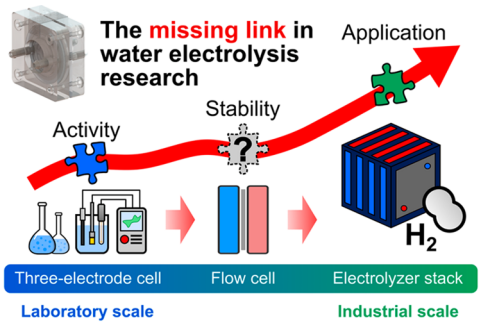

Figure 1. Lab-scale flow electrolyzers provide a robust platform for characterizing electrocatalytic stability, an essential step for the effective scale-up of water electrolysis technologies.

advancement toward meeting industrial requirements. This initial effort aims to establish a straightforward protocol and comparison platform for evaluating and validating electrocatalysts in AWE. We hope this guide facilitates the transition to more realistic testing and promotes rigorous examination of electrocatalytic stability.

Enhancing Electrocatalyst Testing with Lab-Scale Electrolyzers. Upon identifying a promising electrocatalyst in three-electrode cells, flow cells provide a more realistic scenario for further evaluation.[1] Unlike typical three-electrode cells with small electrodes, flow cells accommodate larger electrodes and operate at higher current densities.[2] However, standardizing electrolyzer design is crucial to ensure comparable reaction environments across studies. A significant challenge for flow electrolyzer design is ohmic cell resistance, which can be minimized by compressing two porous electrodes against an ionic conductive separator, resulting in a zero-gap configuration.[3,5,26,29,30] This design shortens ion travel distances and facilitates gas discharge.[13] Despite electrolyte and bubble management being much simpler than similar systems, such as CO_2 electrolyzers,[28] designing zero-gap configurations requires careful consideration of materials, dimensions, and cell architectures. Over the past four years, we have refined various flow cell designs to optimize mass transport, resulting in an optimized architecture.[15] Our group has utilized this configuration to test OER electrocatalysts under realistic AWE conditions.[31−33] As shown in Figure 2a,b, the electrolyzer features rigid plastic flow plates compressing a zero-gap electrode−separator assembly for lab-scale applications with electrode areas of 4 cm^2.

This design is compatible with Ni foam (NF) electrodes, which are popular in AWE research.[34] The electrode preparation is detailed in the Supporting Information. The NF electrodes used have a roughness factor of ∼9.9, estimated from double-layer capacitance measurements in a nonaqueous electrolyte (Figure S1).[35,36] Nickel gauze serves as the current collector, chosen for its alkaline resistance, affordability, and low electrical resistance.[27,37] The flow plates, fabricated from acrylic plastic via computer numerical control (CNC) machining, feature inlet and outlet ports and a pattern directing electrolyte flow through the porous electrode (Figure S2). The assembly uses chemically inert polydimethylsiloxane (PDMS) gaskets, which define the electrode thickness (Figure

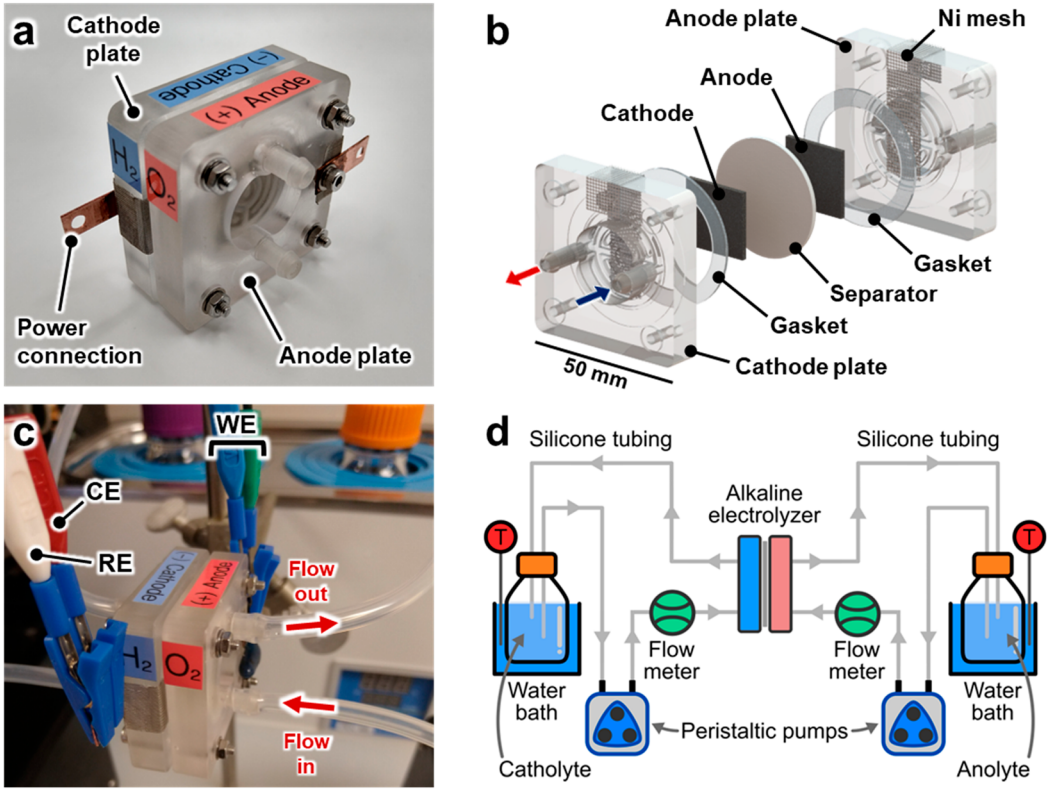

Figure 2. Flow electrolyzer for lab-scale electrocatalyst testing: (a) fully assembled cell, (b) exploded-view rendering of the electrolyzer and its components, (c) electrolyzer under operation, and (d) process flow diagram of the electrolyzer setup.

https://doi.org/10.1021/acsenergylett.3c02758
ACS Energy Lett. 2024, 9, 547−555

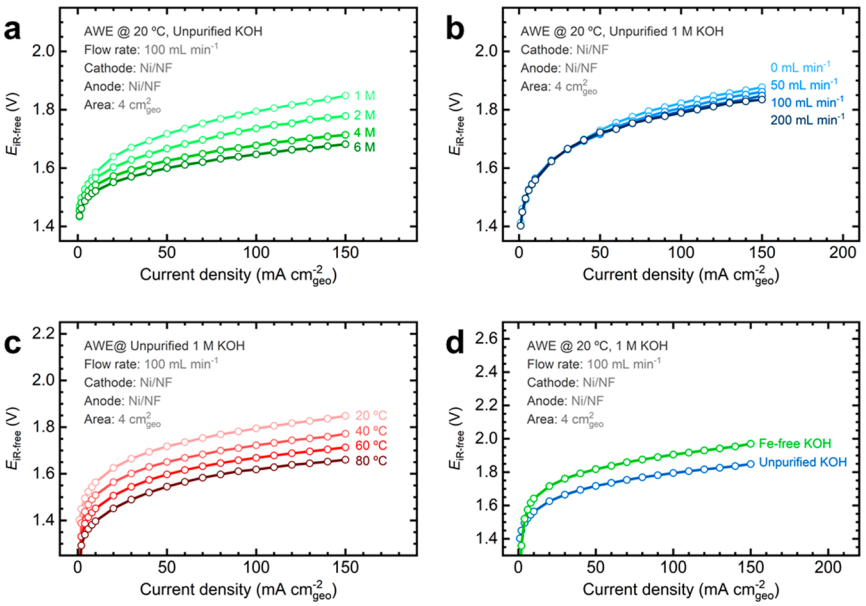

Figure 3. Full-cell polarization curves of the alkaline electrolyzer across various operating conditions: (a) electrolyte concentration, (b) flow rate, (c) temperature, and (d) presence of Fe impurities. Polarization curves were obtained via multistep chronopotentiometry. The *iR*-free cell voltage ($E_{iR\text{-free}}$) is the total cell voltage corrected for *iR* drop using the HFR at each current step.

S3) and seal the current collector to prevent leaks (Figure S4). We use the state-of-the-art Zirfon PERL UTP 500 diaphragm, a well-established and long-lasting standard separator in AWE.[13,27,37] The diaphragm is positioned between the cathode and anode (Figure S5). The manufacture and preparation of these components are detailed in the Supporting Information.

The electrolyzer is assembled using stainless steel bolts tightened uniformly at low torque, creating a compact cell (Figure S6). The bottom-to-top flow direction effectively enhances bubble removal (Figure 2c).[21] The electrolyte temperature was controlled with a water bath and monitored using glass thermometers and stainless-steel thermocouples, with peristaltic pumps circulating the electrolyte through silicone tubing (Figures 2d and S7). This electrolyzer operates in a two-electrode configuration and does not use a reference electrode. Unlike CO_2 electrolysis, where controlling the electrode potential is critical for product selectivity,[28] we aim to emulate a configuration that resembles real-world electrolyzers. A complete guide for conducting electrochemical measurements is included in the Supporting Information, along with best practices and troubleshooting notes.

To prevent uneven gaps, inconsistent pressure distribution, and minimize gas crossover,[13] we optimized this electrolyzer for operation at a maximum current density of 150 mA·cm^{-2}, and the electrode geometric area is limited to 4 cm^2.[26] Note that high current densities, pressures, and temperatures increase gas crossover due to enhanced separator permeability.[2] More advanced electrolyzer designs are advisable for testing practical aspects at higher current densities, including systems with gas−liquid separators, gas detectors, and advanced temperature control. Examples of such robust configurations are available in the literature.[5,21,26,28]

We focus on a simple cell architecture to ease manufacture and minimize operational variables. Components can be fabricated via 3D printing,[38] which offers a quick way to create lightweight, cost-effective electrolyzers.[9,15,33] However, the stability of 3D-printed materials varies significantly.[15] Photoresins, for instance, are brittle and less heat-resistant,[9,38] whereas materials like polyethylene terephthalate glycol (PETG) are more stable but expensive.[9] We advise caution with 3D-printed materials and recommend conventional methods such as CNC machining, especially for materials like polytetrafluoroethylene (PTFE) that are stable in alkaline conditions.[14,39] The 3D models (.stl files) are available in the Supporting Information.

Experimental Conditions Influence Water Electrolysis Performance. We performed electrochemical tests to assess the electrolyzer performance. The measurements and experimental conditions, carefully adapted from previous protocols,[4,9,21,23−25] are detailed in the Supporting Information. We evaluated three electrocatalysts grown on NF substrates: (1) nanostructured Ni and (2) NiFe films prepared by electrodeposition,[40] and (3) Ni_3N precatalysts prepared by thermal oxidation and subsequent nitridation. These materials serve as references: nanostructured nickel serves as a baseline for Ni stability in alkaline media, NiFe is a well-established OER benchmark,[41,42] and Ni_3N represents a promising X-ide precatalyst, extensively studied by our group.[31,32,43,44]

Before performance comparison, the electrolyzer underwent an electrochemical conditioning step at 10 mA·cm^{-2} for 24 h using chronopotentiometry. Polarization curves were derived through multistep chronopotentiometry, holding sequential current steps for 10 min.[21] Currents ranged from 4 to 40 mA (in 4 and 8 mA increments) and 40 to 600 mA (in 40 mA increments), with cell potential recorded at each step before and after conditioning. Electrochemical impedance spectroscopy (EIS) was conducted at each current to determine the high-frequency resistance (HFR), indicative of combined ion and electronic resistances, and used for *iR* correction of polarization curves.[29,45,46] EIS also provided Nyquist plots.

Figure S8 shows the electrochemical tests for the electrolyzer using nanostructured Ni on NF (Ni/NF) electrodes. Conditioning causes significant HFR and Nyquist plot changes due to oxyhydroxide layer formation. Figure S9 compares

https://doi.org/10.1021/acsenergylett.3c02758
ACS Energy Lett. 2024, 9, 547−555

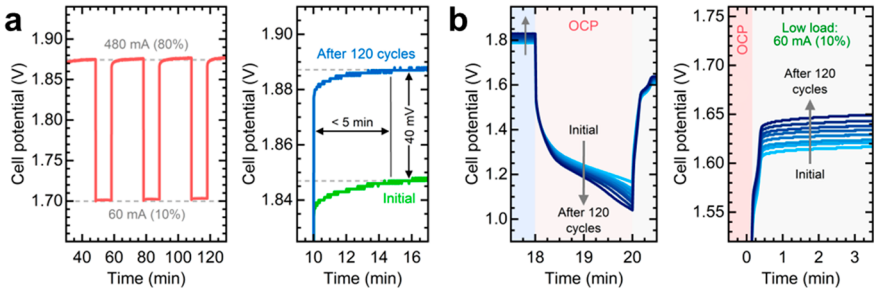

Figure 4. AWE stability testing under variable current and shutdown conditions: (a) close-up views of low- and high-current steps of a Ni_3N anode, and (b) close-up views of shutdown OCP and low-load steps, showcasing cell potential progression over 120 cycles of a NiFe anode.

conditioning responses, Nyquist plots, and polarization curves for bare NF, Ni/NF, and NiFe/NF anodes. NiFe anodes show the lowest cell potential and distinctive Nyquist plot semicircles, indicative of anode and cathode charge transfer resistances. In contrast, Ni/NF surpassed NiFe/NF as the cathode (Figure S10). Next, we examined the performance of the Ni_3N precatalyst as cathode and anode (Figure S11). Despite the activity improvement of Ni_3N during conditioning, activated Ni/NF still surpassed it in both roles. These changes are attributed to in situ Ni oxyhydroxide formation during the OER, a process our group has extensively studied.[31,32,43,44,47] Thus, conditioning is crucial to achieve a stable active phase.

After identifying promising electrocatalysts, testing under industrially relevant conditions becomes critical.[14,48] We evaluated four critical AWE conditions that impact the membrane−electrode assembly environment:[21] electrolyte concentration, liquid flow rate, temperature, and presence of Fe impurities, with results depicted in Figure 3. This electrolyzer operates at ambient pressure, as high-pressure setups are complex and costly, sometimes impractical for laboratory environments.[4] Given our operating current densities, pressure impact is minor compared to temperature or electrolyte concentration effects.[23] However, we advise using more advanced electrolysis setups to simulate industrial conditions.[5,21,26,28]

Higher electrolyte concentrations decrease the ohmic resistance.[4] Moreover, increased viscosity leads to hydrodynamics akin to industrial electrolyzers, enhancing the realism of bubble management.[37] We tested up to 6 M KOH (between 25 and 30 wt %), which lies close to the highest ionic conductivity for KOH.[3,5,37] Figure 3a shows lower cell potentials with higher concentrations, mainly due to decreased cell resistance, with HFR dropping from ∼1.1 to ∼0.5 $\Omega \cdot cm^2$ between 1 and 6 M KOH (Figure S12b). Faster oxyhydroxide phase aging explains the differences in conditioning responses and Nyquist plots at higher concentrations.[39,49]

Forced convection is essential at high currents to manage increased water and gas production, impacting mass transport.[30,50] Polarization curves diverge at current densities exceeding ∼50 $mA \cdot cm^{-2}$ (Figure 3b), and the HFR decreases from ∼1.3 to ∼1.1 $\Omega \cdot cm^2$ with higher flow rates (Figure S13). As shown in Figure S13g, higher flow rates lower the cell potential (∼115 mV) and stabilize current responses due to effective bubble removal.[27,33] Note that doubling the flow rate from 100 to 200 $mL \cdot min^{-1}$ only lowers cell potential by 15%, highlighting the importance of pump efficiency on operating costs. Thus, selecting an optimal flow rate to balance stability and minimize ohmic resistance is vital.[27] We used a 100 $mL \cdot min^{-1}$ flow rate in later experiments.

High temperatures enhance electrode kinetics, electrolyte conductivity, and gas removal, making them preferable in industrial settings.[37,51] Consistent temperature control is crucial as fluctuations can change material properties, cause corrosion, or modify reaction rates.[52] However, many electrocatalytic stability studies often overlook temperature's role. We tested the electrolyzer performance between 20 and 80 °C, setting 80 °C as the upper limit to avoid excessive damage and minimize corrosion.[3] Increasing temperature reduces the cell potential by about 200 mV from 20 to 80 °C at 150 $mA \cdot cm^{-2}$ (Figure 3c), with the HFR dropping to 0.7 $\Omega \cdot cm^{-2}$ at 80 °C (Figure S14), the most significant impact on the HFR compared to electrolyte concentration and flow rate.

Metal impurities are critical in AWE research. Following de Groot's classification,[48] we tested the electrolyzer performance under "iron-free" and "some-iron" scenarios. The Ni/NF anode exhibits higher cell potentials with Fe-purified KOH electrolytes (Figure 3d), consistent with the well-known effects of Fe incorporation.[17,39,49,53] Differences in HFR suggest that Fe impurities influence cell resistance (Figure S15). We agree that Fe-free electrolyzers suit fundamental research and initial electrocatalyst screening. However, real-world applications involve Fe impurities, often introduced via feedwater or corrosion.[1,48] Thus, we used unpurified KOH in later experiments to show consistency with the presence of Fe.[17,48] Note, however, that our design is compatible with Fe-free testing, and impurity effects can be quantified. Best practices in electrolyte preparation and control tests are advised to address impurity effects.[39] While impurity considerations depend on the research aim, their assessment is crucial for electrocatalyst testing.[52]

Unlocking Next-Level Stability Testing with Variable Loads. Electrode stability significantly influences the lifetime and operational costs of AWE systems.[20] However, many studies focus primarily on electrocatalytic activity, often overlooking or inadequately investigating stability.[52] Testing protocols often use shorter timeframes and lower current densities than industrial needs,[51] failing to mimic real industrial AWE electrolyzer conditions, particularly under intermittent renewable power sources.[54] Thus, there is a need for accelerated degradation tests that accurately simulate degradation mechanisms over appropriate time scales and realistic operating conditions to develop more robust electrocatalysts.

Using variable current and simulated shutdown steps stresses the electrodes and speeds up degradation. Thus, testing fluctuating currents is an excellent approach to assessing catalyst adaptability.[4,23] Inspired by previous approaches,[20,24,54,55] we implemented two stability protocols to evaluate our three electrocatalytic materials. The electro-

https://doi.org/10.1021/acsenergylett.3c02758
ACS Energy Lett. 2024, 9, 547−555

lyzer, operating in unpurified 6 M KOH at 50 °C with a 100 $mL \cdot min^{-1}$ flow rate, followed conditions similar to state-of-the-art alkaline electrolyzers (HFR ~ 0.4 $\Omega \cdot cm^2$).[13] Electrodes underwent conditioning for 24 h before testing. Figure S16 shows Ni/NF electrodes stabilizing in approximately 18 h, attributed to NiOOH film formation and Fe incorporation.[17,47]

Our first stability test alternated between low (60 mA for 10 min) and high (480 mA for 20 min) current steps, each cycle lasting 30 min, repeated 120 times for a total of 60 h (Figure 4a). These steps represent 10% and 80% of the potentiostat's maximum current capacity. Electrodes can undergo reverse currents and undesirable transformations during electrolyzer shutdown.[37,54] Thus, our second stability test combines fluctuating current and shutdown steps (Figure 4b), incorporating an open-circuit potential (OCP) step for 2 min between high and low currents (Figure S25b). For both tests, we measured the HFR after each cycle using galvanostatic EIS and recorded polarization and Nyquist plots before and after the 120 cycles. Results with Ni/NF, NiFe/NF, and Ni_3N/NF anodes are detailed in the Supporting Information (Figures S17−S28), including supporting notes describing important transformations observed for each electrocatalyst. Additionally, Tables S1 and S2 summarize the performance metrics for the fluctuating current and reverse current tests, respectively. Electrochemical characterization of these electrodes conducted at the three-electrode cell level is available in previous studies.[32,39,44]

We do not extensively discuss the deactivation or self-healing mechanisms of the electrocatalysts evaluated here but encourage further exploration of the following aspects:

Electrochemical Conditioning. Our results underscore the significance of conditioning in AWE. Unlike PEM electrolysis, where conditioning is typically shorter,[11,21] longer conditioning times are recommended to achieve complete electrocatalyst transformation.[12,54,56] Conditioning might require several hours to form the most stable phase, and the duration might vary for different precatalysts.[27] This step also serves as a warming-up period[21,27] and stabilizes Fe incorporation and dissolution.[48] Note that in situ reconstruction during conditioning could lead to catalyst dissolution and mechanical degradation, impacting stability.[6] Therefore, conditioning also serves to identify electrocatalysts unable to achieve steady responses before conducting stability tests. Considering these insights, we advise conducting electrochemical conditioning for at least 12 h to ensure uniform testing conditions and improve reproducibility in AWE research.

EIS for Electrolyzer Evaluation. EIS is a powerful tool for tracking electrolyzer performance. Tracking the HFR reveals conductivity changes, including those from material transformations (i.e., electronic) or bubble evolution (i.e., ionic). EIS can also detect charge transfer resistance shifts when one electrode is altered, aiding Nyquist plot interpretation. However, interpreting full-cell Nyquist plots can be complex, and caution is advised. Tafel analysis of *iR*-free polarization curves at low current densities can offer comparative kinetic insights.[5,46]

Catalyst Deactivation and Dissolution. Our stability protocols help assess electrocatalyst resilience against operational instability from current or potential fluctuations.[18,19] Our findings suggest that catalyst degradation often progresses slowly, avoiding abrupt performance loss or failure (see Figure S25). Simulated shutdown tests reveal gradual cell potential shifts, potentially forming soluble metal species (see Figure S23).[37] Thus, shutdown stability tests can aid in tracking corrosion and catalyst dissolution, as well as related effects such as membrane poisoning.

Effects of Operating Environments. It is crucial to study systematically temperature and concentration effects, as these can alter catalyst dissolution and kinetics.[4,18,51] Electronic conductivity is another aspect requiring further exploration.[20,22] For example, NiFe oxyhydroxides are effective OER catalysts in AWE, while NiCo oxides perform better in AEM electrolysis due to better conductivity.[12] Do not assume catalyst stability in all environments.

Coupling with Characterization Techniques. Researchers are encouraged to integrate these protocols with in situ and ex situ analyses to understand catalyst deactivation comprehensively.[48,52] Use elemental analysis to monitor metal dissolution, particularly during intermittent operation. Analyzing separators post-mortem, alongside HFR and physicochemical analysis, helps assess membrane poisoning.[1,52] Complement these with faradaic efficiency assessments[41,57] and investigations on practical aspects like gas crossover and purity.[5,26]

Catalyst Integrity and Mechanical Stability. Often overlooked at the lab scale, catalyst integrity is crucial in realistic settings. Intermittent operation tests can be utilized to measure the impact of bubble evolution on catalyst adhesion.[2,33] Our electrolyzer setup is ideal for testing new electrode designs or pore engineering techniques to enhance bubble release and mechanical stability.[33]

Strategies for Catalyst Resilience. Future studies should explore strategies such as using sacrificial electrodes,[20] analyzing shutdown step duration, applying cathodic currents,[54] or using transient voltage steps for phase regeneration after reverse currents.[18] Bifunctional materials with inherent resilience to reverse currents are also attractive.[4]

Electrocatalyst Research Needs Standardized Protocols. In addition to standardized testing setups, the AWE community urgently needs protocols and guidelines for meaningful electrocatalytic performance comparison across laboratories.[1,21,58] This endeavor requires strong collaboration between academia and industry to ensure reproducible, fair, and relevant benchmarking.[41,52,59] Drawing inspiration from the fuel cell field, which has made strides through standardization,[21−23] AWE benchmarking should clearly define operating conditions, testing procedures, evaluation criteria, and establish "gold" standards.[21,41]

As an initial step toward AWE benchmarking, we propose a protocol for evaluating electrocatalytic material stability using lab-scale electrolyzers (Figure 5), including workflows for stability testing under fluctuating currents and shutdown conditions (Schemes S1 and S2). These are adapted from benchmarking efforts in the AWE community, PEM electrolysis, and fuel cell research.[10,11,21,24,25,55,60] We include an example of a potentiostat sequence to conduct these workflows systematically (Figure S29). Moreover, an in-depth description of the characterization techniques recommended for evaluating electrocatalytic stability, along with the specific insights each technique offers, can be found in our previous work.[43] Following Risch's benchmarking criteria,[41] we encourage AWE researchers to evaluate electrocatalytic stability under specified conditions (i.e., 50 °C, unpurified 6 M KOH, 100 $mL \cdot cm^{-1}$ flow rate), using Ni and NiFe as standards. Our lab-scale electrolyzer offers an accessible platform for evaluating electrocatalytic stability under realistic conditions.

https://doi.org/10.1021/acsenergylett.3c02758
ACS Energy Lett. 2024, 9, 547−555

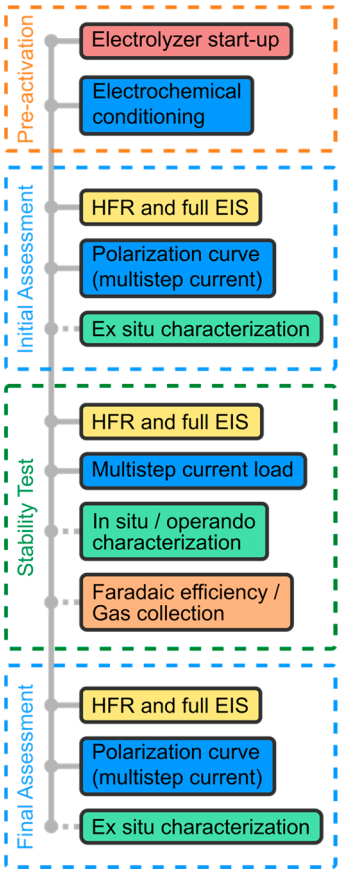

Figure 5. Flowchart depicting the standard protocol for evaluating electrocatalytic stability in lab-scale electrolyzers.

Defining meaningful evaluation criteria is essential and requires further attention. We note six key considerations for evaluating performance: (1) Focus on deactivation rates rather than stability duration or activity.[19,27] Suitable metrics include the activity-stability factor,[61] the S-number,[1,41] or the reverse-current stability factor.[20] (2) Reaction environments and setups must be reported in detail, using reference materials for comparison. (3) Focus on understanding catalyst deactivation and failure mechanisms over merely reporting stabilities. (4) Expose electrocatalysts to challenging environments, especially under claims of "exceptional" stability. Although steady-state conditions aid initial development,[1] intermittent operation truly tests catalyst resilience.[4] (5) Ensure reproducibility and evaluate uncertainty.[21,39,41] (6) Use *iR*-free polarization curves to compare electrocatalytic activity and HFR to determine, compare, and monitor cell resistance, equivalent to *iR* compensation measurements in three-electrode cells.[62,63]

This protocol is merely a starting point, necessitating further refinement. We encourage complementing this guide with resources on electrolyzer disassembly for ex situ characterization,[16] electrolyzer troubleshooting,[28,58] methods for preparing and characterizing separators and diffusion layers,[50,58,64−66] and resources for other bipolar electrolyzer technologies.[58,64] As depicted in Figure 5, ex situ characterization after the initial assessment is encouraged to identify the most stable phase following preactivation and facilitate comparisons of structure and chemical compositions before and after the stability test. Note that destructive ex situ characterization techniques require separate electrocatalyst samples. For custom cell construction, we recommend following our method to characterize the hydrodynamics and mass transport.[15] More protocols are necessary for specific electrolyzer evaluations, including separator stability and degradation mechanism studies.[13,16,23] We hope our work inspires further standardization efforts, advancing toward a comprehensive comparison platform in AWE.

Concluding Remarks. Electrocatalyst research in AWE needs to shift from focusing solely on high performance under impractical conditions to understanding physical phenomena in realistic settings.[4] The industry favors efficient, cost-effective materials over those with merely "ultralow" overpotentials.[22] Researchers should design catalysts carefully, avoiding complex chemistries that might lead to instability or harmful byproducts affecting components like separators. High activity alone should not be the only performance measure; broader aspects need consideration.[27,29]

Future strategic directions include exploring catalyst resilience to electrolyte convection,[2] designing electrodes with enhanced bubble removal,[33] and examining the impact of high temperatures on performance.[4,21] Other improvement areas include zero-gap configuration and electrolyzer components, focusing on separator properties, gas crossover, impurity effects, flow plate design, and component wear.[2,13,22,26,48] Understanding catalyst deactivation is essential for addressing durability challenges,[52] and research should focus on improving resilience to fluctuating currents.[4,54] Collaborative efforts between academia and industry are crucial for setting appropriate equipment, operational methods, and evaluation protocols.

Our lab-scale electrolyzer and stability protocols provide opportunities for significant AWE research. We invite the community to use our guidelines for evaluating electrocatalytic stability after preliminary catalyst screenings in traditional three-electrode setups. Following these protocols will foster more accurate and consistent comparisons of electrocatalytic performance. While our motivation is to meet industry needs, there is still a significant journey to bridge the gap between academia and industry. We urge future studies to continue this effort and promote collaboration with industry to advance AWE research.

Raul A. Marquez orcid.org/0000-0003-3885-5007
Michael Espinosa orcid.org/0000-0002-9457-574X
Emma Kalokowski orcid.org/0009-0000-5264-8464
Yoon Jun Son orcid.org/0000-0003-1704-2314
Kenta Kawashima orcid.org/0000-0001-7318-6115
Thuy Vy Le orcid.org/0009-0004-1422-1450
Chikaodili E. Chukwuneke orcid.org/0000-0003-0478-8387
C. Buddie Mullins orcid.org/0000-0003-1030-4801

■ ASSOCIATED CONTENT

Supporting Information

The Supporting Information is available free of charge at https://pubs.acs.org/doi/10.1021/acsenergylett.3c02758.

Materials and methods; guidelines on electrolyzer materials, fabrication, assembly, and operation; electrochemical measurements; troubleshooting notes; and supporting figures (PDF)

Lab-scale electrolyzer assembly procedure (MP4)

3D CAD models (stl files) of the electrolyzer flow plates and barb fittings (ZIP)

https://doi.org/10.1021/acsenergylett.3c02758
ACS Energy Lett. 2024, 9, 547−555

AUTHOR INFORMATION

Complete contact information is available at:
https://pubs.acs.org/10.1021/acsenergylett.3c02758

Author Contributions

The manuscript was written through the contributions of all authors. All authors have approved the final version of the manuscript.

Notes

Views expressed in this Viewpoint are those of the authors and not necessarily the views of the ACS.
The authors declare no competing financial interest.

ACKNOWLEDGMENTS

The authors gratefully acknowledge funding from the National Science Foundation (NSF) via Grant CHE-2102307 and the Welch Foundation through Grant F-1436 for their generous support. R.A.M. (CVU 919871) acknowledges CONAHCYT for his Doctoral scholarship award. We thank David Gray and Shallaco McDonald for manufacturing the electrolyzer flow plates and conducting leakage tests.

REFERENCES

(1) Edgington, J.; Seitz, L. C. Advancing the Rigor and Reproducibility of Electrocatalyst Stability Benchmarking and Intrinsic Material Degradation Analysis for Water Oxidation. *ACS Catal.* **2023**, *13*, 3379−3394.
(2) Domalanta, M. R.; Bamba, J. N.; Matienzo, D. D.; del Rosario-Paraggua, J. A.; Ocon, J. Pathways towards Achieving High Current Density Water Electrolysis: From Material Perspective to System Configuration. *ChemSusChem* **2023**, *16* (13), No. e202300310.
(3) de Groot, M. T.; Kraakman, J.; Garcia Barros, R. L. Optimal Operating Parameters for Advanced Alkaline Water Electrolysis. *Int. J. Hydrogen Energy* **2022**, *47* (82), 34773−34783.
(4) Ehlers, J. C.; Feidenhans'l, A. A.; Therkildsen, K. T.; Larrazábal, G. O. Affordable Green Hydrogen from Alkaline Water Electrolysis: Key Research Needs from an Industrial Perspective. *ACS Energy Lett.* **2023**, *8*, 1502−1509.
(5) Ju, W.; Heinz, M. V. F.; Pusterla, L.; Hofer, M.; Fumey, B.; Castiglioni, R.; Pagani, M.; Battaglia, C.; Vogt, U. F. Lab-Scale Alkaline Water Electrolyzer for Bridging Material Fundamentals with Realistic Operation. *ACS Sustainable Chem. Eng.* **2018**, *6* (4), 4829−4837.
(6) Wan, L.; Xu, Z.; Xu, Q.; Pang, M.; Lin, D.; Liu, J.; Wang, B. Key Components and Design Strategy of the Membrane Electrode Assembly for Alkaline Water Electrolysis. *Energy Environ. Sci.* **2023**, *16*, 1384.
(7) Kamat, P. V. 2022 Citation Analysis and Impact of Energy Journals. *ACS Energy Lett.* **2023**, *8* (8), 3646−3648.
(8) Jin, S. Fewer Sandwich Papers, Please. *ACS Energy Lett.* **2022**, *7* (10), 3727−3728.
(9) Browne, M. P.; Dodwell, J.; Novotny, F.; Jaśkaniec, S.; Shearing, P. R.; Nicolosi, V.; Brett, D. J. L.; Pumera, M. Oxygen Evolution Catalysts under Proton Exchange Membrane Conditions in a Conventional Three Electrode Cell vs. Electrolyser Device: A Comparison Study and a 3D-Printed Electrolyser for Academic Labs. *J. Mater. Chem. A* **2021**, *9* (14), 9113−9123.
(10) Jiménez, P. C.; Wiberg, G. K. H.; Sievers, G. W.; Brüser, V.; Arenz, M. Bridging the Gap between Basic Research and Application: A Half-Cell Setup for High Current Density Measurements of Ir-Based Oxygen Evolution Reaction Catalysts on Porous Transport Electrodes. *J. Mater. Chem. A* **2023**, *11* (37), 20129−20138.
(11) Geuß, M.; Milosevic, M.; Bierling, M.; Löttert, L.; Abbas, D.; Escalera-López, D.; Lloret, V.; Ehelebe, K.; Mayrhofer, K. J. J.; Thiele, S.; Cherevko, S. Investigation of Iridium-Based OER Catalyst Layers in a GDE Half-Cell Setup: Opportunities and Challenges. *J. Electrochem. Soc.* **2023**, *170* (11), 114510.
(12) Xu, D.; Stevens, M. B.; Cosby, M. R.; Oener, S. Z.; Smith, A. M.; Enman, L. J.; Ayers, K. E.; Capuano, C. B.; Renner, J. N.; Danilovic, N.; Li, Y.; Wang, H.; Zhang, Q.; Boettcher, S. W. Earth-Abundant Oxygen Electrocatalysts for Alkaline Anion-Exchange-Membrane Water Electrolysis: Effects of Catalyst Conductivity and Comparison with Performance in Three-Electrode Cells. *ACS Catal.* **2019**, *9* (1), 7−15.
(13) Aili, D.; Kraglund, M. R.; Rajappan, S. C.; Serhiichuk, D.; Xia, Y.; Deimede, V.; Kallitsis, J.; Bae, C.; Jannasch, P.; Henkensmeier, D.; Jensen, J. O. Electrode Separators for the Next-Generation Alkaline Water Electrolyzers. *ACS Energy Lett.* **2023**, *8* (4), 1900−1910.
(14) Thissen, N.; Hoffmann, J.; Tigges, S.; Vogel, D. A. M.; Thoede, J. J.; Khan, S.; Schmitt, N.; Heumann, S.; Etzold, B. J. M.; Mechler, A. K. Industrially Relevant Conditions in Lab-Scale Analysis for Alkaline Water Electrolysis. *ChemElectroChem* **2024**, *11* (1), e202300432 DOI: 10.1002/celc.202300432.
(15) Márquez-Montes, R. A.; Collins-Martínez, V. H.; Pérez-Reyes, I.; Chávez-Flores, D.; Graeve, O. A.; Ramos-Sánchez, V. H. Electrochemical Engineering Assessment of a Novel 3D-Printed Filter-Press Electrochemical Reactor for Multipurpose Laboratory Applications. *ACS Sustainable Chem. Eng.* **2020**, *8* (9), 3896−3905.
(16) Glenn, J. R.; Lindquist, G. A.; Roberts, G. M.; Boettcher, S. W.; Ayers, K. E. Standard Operating Procedure for Post-Operation Component Disassembly and Observation of Benchtop Water Electrolyzer Testing. *Front. Energy Res.* **2022**, *10*, 01.
(17) Demnitz, M.; Lamas, Y. M.; Garcia Barros, R. L.; de Leeuw den Bouter, A.; van der Schaaf, J.; Theodorus de Groot, M. Effect of Iron Addition to the Electrolyte on Alkaline Water Electrolysis Performance. *iScience* **2024**, *27*, 108695.
(18) Xie, X.; Du, L.; Yan, L.; Park, S.; Qiu, Y.; Sokolowski, J.; Wang, W.; Shao, Y. Oxygen Evolution Reaction in Alkaline Environment: Material Challenges and Solutions. *Adv. Funct. Mater.* **2022**, *32* (21), 2110036.
(19) Scott, S. L. A Matter of Life(time) and Death. *ACS Catal.* **2018**, *8* (9), 8597−8599.
(20) Kim, Y.; Jung, S.-M.; Kim, K.-S.; Kim, H.-Y.; Kwon, J.; Lee, J.; Cho, H.-S.; Kim, Y.-T. Cathodic Protection System against a Reverse-Current after Shut-Down in Zero-Gap Alkaline Water Electrolysis. *JACS Au* **2022**, *2* (11), 2491−2500.
(21) Bender, G.; Carmo, M.; Smolinka, T.; Gago, A.; Danilovic, N.; Mueller, M.; Ganci, F.; Fallisch, A.; Lettenmeier, P.; Friedrich, K. A.; Ayers, K.; Pivovar, B.; Mergel, J.; Stolten, D. Initial Approaches in Benchmarking and Round Robin Testing for Proton Exchange Membrane Water Electrolyzers. *Int. J. Hydrogen Energy* **2019**, *44* (18), 9174−9187.
(22) Ayers, K.; Danilovic, N.; Ouimet, R.; Carmo, M.; Pivovar, B.; Bornstein, M. Perspectives on Low-Temperature Electrolysis and Potential for Renewable Hydrogen at Scale. *Annu. Rev. Chem. Biomol. Eng.* **2019**, *10* (1), 219−239.
(23) Ren, Z.; Wang, J.; Yu, Z.; Zhang, C.; Gao, S.; Wang, P. Experimental Studies and Modeling of a 250-kW Alkaline Water Electrolyzer for Hydrogen Production. *J. Power Sources* **2022**, *544*, 231886.
(24) Tsotridis, G.; Pilenga, A. *EU Harmonized Protocols for Testing of Low Temperature Water Electrolysis*; European Commission, Joint Research Centre, Publications Office, 2021. DOI: 10.2760/502481.
(25) Malkow, T.; Pilenga, A.; Tsotridis, G.; De Marco, G. *EU Harmonised Polarisation Curve Test Method for Low-Temperature Water Electrolysis*; Publications Office of the European Union, 2018. DOI: 10.2760/179509.
(26) Lira Garcia Barros, R.; Kraakman, J. T.; Sebregts, C.; van der Schaaf, J.; de Groot, M. T. Impact of an Electrode-Diaphragm Gap on Diffusive Hydrogen Crossover in Alkaline Water Electrolysis. *Int. J. Hydrogen Energy* **2024**, *49*, 886.
(27) Karacan, C.; Lohmann-Richters, F. P.; Keeley, G. P.; Scheepers, F.; Shviro, M.; Müller, M.; Carmo, M.; Stolten, D. Challenges and

Important Considerations When Benchmarking Single-Cell Alkaline Electrolyzers. *Int. J. Hydrogen Energy* **2022**, *47* (7), 4294−4303.
(28) Iglesias van Montfort, H.-P.; Subramanian, S.; Irtem, E.; Sassenburg, M.; Li, M.; Kok, J.; Middelkoop, J.; Burdyny, T. An Advanced Guide to Assembly and Operation of CO2 Electrolyzers. *ACS Energy Lett.* **2023**, *8*, 4156−4161.
(29) Phillips, R.; Dunnill, C. W. Zero Gap Alkaline Electrolysis Cell Design for Renewable Energy Storage as Hydrogen Gas. *RSC Adv.* **2016**, *6* (102), 100643−100651.
(30) Schalenbach, M.; Kasian, O.; Mayrhofer, K. J. J. An Alkaline Water Electrolyzer with Nickel Electrodes Enables Efficient High Current Density Operation. *Int. J. Hydrogen Energy* **2018**, *43* (27), 11932−11938.
(31) Marquez-Montes, R. A.; Kawashima, K.; Son, Y. J.; Weeks, J. A.; Sun, H. H.; Celio, H.; Ramos-Sánchez, V. H.; Mullins, C. B. Mass Transport-Enhanced Electrodeposition of Ni−S−P−O Films on Nickel Foam for Electrochemical Water Splitting. *J. Mater. Chem. A* **2021**, *9*, 7736−7749.
(32) Kawashima, K.; Márquez-Montes, R. A.; Li, H.; Shin, K.; Cao, C. L.; Vo, K. M.; Son, Y. J.; Wygant, B. R.; Chunangad, A.; Youn, D. H.; Henkelman, G.; Ramos-Sánchez, V. H.; Mullins, C. B. Electrochemical Behavior of a Ni3N OER Precatalyst in Fe-Purified Alkaline Media: The Impact of Self-Oxidation and Fe Incorporation. *Mater. Adv.* **2021**, *2*, 2299−2309.
(33) Márquez, R. A.; Kawashima, K.; Son, Y. J.; Rose, R.; Smith, L. A.; Miller, N.; Carrasco Jaim, O. A.; Celio, H.; Mullins, C. B. Tailoring 3D-Printed Electrodes for Enhanced Water Splitting. *ACS Appl. Mater. Interfaces* **2022**, *14* (37), 42153−42170.
(34) Zheng, W.; Liu, M.; Lee, L. Y. S. Best Practices in Using Foam-Type Electrodes for Electrocatalytic Performance Benchmark. *ACS Energy Lett.* **2020**, *5*, 3260−3264.
(35) Yoon, Y.; Yan, B.; Surendranath, Y. Suppressing Ion Transfer Enables Versatile Measurements of Electrochemical Surface Area for Intrinsic Activity Comparisons. *J. Am. Chem. Soc.* **2018**, *140* (7), 2397−2400.
(36) Morales, D. M.; Risch, M. Seven Steps to Reliable Cyclic Voltammetry Measurements for the Determination of Double Layer Capacitance. *J. Phys. Energy* **2021**, *3* (3), 034013.
(37) Schalenbach, M.; Zeradjanin, A.; Kasian, O.; Cherevko, S.; Mayrhofer, K. A Perspective on Low-Temperature Water Electrolysis − Challenges in Alkaline and Acidic Technology. *Int. J. Electrochem. Sci.* **2018**, *13*, 1173−1226.
(38) Chisholm, G.; Kitson, P. J.; Kirkaldy, N. D.; Bloor, L. G.; Cronin, L. 3D Printed Flow Plates for the Electrolysis of Water: An Economic and Adaptable Approach to Device Manufacture. *Energy Environ. Sci.* **2014**, *7* (9), 3026−3032.
(39) Márquez, R. A.; Kawashima, K.; Son, Y. J.; Castelino, G.; Miller, N.; Smith, L. A.; Chukwuneke, C. E.; Mullins, C. B. Getting the Basics Right: Preparing Alkaline Electrolytes for Electrochemical Applications. *ACS Energy Lett.* **2023**, *8* (2), 1141−1146.
(40) Hoang, T. T. H.; Gewirth, A. A. High Activity Oxygen Evolution Reaction Catalysts from Additive-Controlled Electrodeposited Ni and NiFe Films. *ACS Catal.* **2016**, *6* (2), 1159−1164.
(41) Risch, M. Reporting Activities for the Oxygen Evolution Reaction. *Commun. Chem.* **2023**, *6* (1), 1−5.
(42) McCrory, C. C. L.; Jung, S.; Peters, J. C.; Jaramillo, T. F. Benchmarking Heterogeneous Electrocatalysts for the Oxygen Evolution Reaction. *J. Am. Chem. Soc.* **2013**, *135* (45), 16977−16987.
(43) Kawashima, K.; Marquez, R. A.; Smith, L. A.; Vaidyula, R. R.; Carrasco Jaim, O. A.; Wang, Z.; Son, Y. J.; Cao, C. L.; Mullins, C. B. A Review of Transition Metal Boride, Carbide, Pnictide, and Chalcogenide Water Oxidation Electrocatalysts. *Chem. Rev.* **2023**, *123* (23), 12795−13208.
(44) Chukwuneke, C. E.; Kawashima, K.; Li, H.; Marquez, R. A.; Son, Y. J.; Smith, L. A.; Celio, H.; Henkelman, G.; Mullins, C. B. Electrochemically Engineered Domain: Nickel−Hydroxide/Nickel Nitride Composite for Alkaline HER Electrocatalysis. *J. Mater. Chem. A* **2024**, *12*, 1654.
(45) Bernt, M.; Gasteiger, H. A. Influence of Ionomer Content in IrO2/TiO2 Electrodes on PEM Water Electrolyzer Performance. *J. Electrochem. Soc.* **2016**, *163* (11), F3179.
(46) Möckl, M.; Ernst, M. F.; Kornherr, M.; Allebrod, F.; Bernt, M.; Byrknes, J.; Eickes, C.; Gebauer, C.; Moskovtseva, A.; Gasteiger, H. A. Durability Testing of Low-Iridium PEM Water Electrolysis Membrane Electrode Assemblies. *J. Electrochem. Soc.* **2022**, *169* (6), 064505.
(47) Son, Y. J.; Kim, S.; Leung, V.; Kawashima, K.; Noh, J.; Kim, K.; Marquez, R. A.; Carrasco-Jaim, O. A.; Smith, L. A.; Celio, H.; Milliron, D. J.; Korgel, B. A.; Mullins, C. B. Effects of Electrochemical Conditioning on Nickel-Based Oxygen Evolution Electrocatalysts. *ACS Catal.* **2022**, *12* (16), 10384−10399.
(48) de Groot, M. T. Alkaline Water Electrolysis: With or without Iron in the Electrolyte? *Curr. Opin. Chem. Eng.* **2023**, *42*, 100981.
(49) Klaus, S.; Cai, Y.; Louie, M. W.; Trotochaud, L.; Bell, A. T. Effects of Fe Electrolyte Impurities on Ni(OH)2/NiOOH Structure and Oxygen Evolution Activity. *J. Phys. Chem. C* **2015**, *119* (13), 7243−7254.
(50) Ouimet, R. J.; Young, J. L.; Schuler, T.; Bender, G.; Roberts, G. M.; Ayers, K. E. Measurement of Resistance, Porosity, and Water Contact Angle of Porous Transport Layers for Low-Temperature Electrolysis Technologies. *Front. Energy Res.* **2022**, *10*, 911077.
(51) Lohmann-Richters, F. P.; Renz, S.; Lehnert, W.; Müller, M.; Carmo, M. Review—Challenges and Opportunities for Increased Current Density in Alkaline Electrolysis by Increasing the Operating Temperature. *J. Electrochem. Soc.* **2021**, *168* (11), 114501.
(52) Nguyen, H. L.; Han, J.; Nguyen, X. L.; Yu, S.; Goo, Y.-M.; Le, D. D. Review of the Durability of Polymer Electrolyte Membrane Fuel Cell in Long-Term Operation: Main Influencing Parameters and Testing Protocols. *Energies* **2021**, *14* (13), 4048.
(53) Trotochaud, L.; Young, S. L.; Ranney, J. K.; Boettcher, S. W. Nickel−Iron Oxyhydroxide Oxygen-Evolution Electrocatalysts: The Role of Intentional and Incidental Iron Incorporation. *J. Am. Chem. Soc.* **2014**, *136* (18), 6744−6753.
(54) Abdel Haleem, A.; Nagasawa, K.; Kuroda, Y.; Nishiki, Y.; Zaenal, A.; Mitsushima, S. A New Accelerated Durability Test Protocol for Water Oxidation Electrocatalysts of Renewable Energy Powered Alkaline Water Electrolyzers. *Electrochemistry* **2021**, *89* (2), 186−191.
(55) Weiß, A.; Siebel, A.; Bernt, M.; Shen, T.-H.; Tileli, V.; Gasteiger, H. A. Impact of Intermittent Operation on Lifetime and Performance of a PEM Water Electrolyzer. *J. Electrochem. Soc.* **2019**, *166* (8), F487.
(56) Wygant, B. R.; Kawashima, K.; Mullins, C. B. Catalyst or Precatalyst? The Effect of Oxidation on Transition Metal Carbide, Pnictide, and Chalcogenide Oxygen Evolution Catalysts. *ACS Energy Lett.* **2018**, *3* (12), 2956−2966.
(57) Kempler, P. A.; Nielander, A. C. Reliable Reporting of Faradaic Efficiencies for Electrocatalysis Research. *Nat. Commun.* **2023**, *14* (1), 1158.
(58) Rios Amador, I.; Hannagan, R. T.; Marin, D. H.; Perryman, J. T.; Rémy, C.; Hubert, M. A.; Lindquist, G. A.; Chen, L.; Stevens, M. B.; Boettcher, S. W.; Nielander, A. C.; Jaramillo, T. F. Protocol for Assembling and Operating Bipolar Membrane Water Electrolyzers. *STAR Protocols* **2023**, *4* (4), 102606.
(59) Bligaard, T.; Bullock, R. M.; Campbell, C. T.; Chen, J. G.; Gates, B. C.; Gorte, R. J.; Jones, C. W.; Jones, W. D.; Kitchin, J. R.; Scott, S. L. Toward Benchmarking in Catalysis Science: Best Practices, Challenges, and Opportunities. *ACS Catal.* **2016**, *6* (4), 2590−2602.
(60) Aßmann, P.; Gago, A. S.; Gazdzicki, P.; Friedrich, K. A.; Wark, M. Toward Developing Accelerated Stress Tests for Proton Exchange Membrane Electrolyzers. *Curr. Opin. Electrochem.* **2020**, *21*, 225−233.
(61) Kim, Y.-T.; Lopes, P. P.; Park, S.-A.; Lee, A.-Y.; Lim, J.; Lee, H.; Back, S.; Jung, Y.; Danilovic, N.; Stamenkovic, V.; Erlebacher, J.; Snyder, J.; Markovic, N. M. Balancing Activity, Stability and Conductivity of Nanoporous Core-Shell Iridium/Iridium Oxide Oxygen Evolution Catalysts. *Nat. Commun.* **2017**, *8* (1), 1449.

https://doi.org/10.1021/acsenergylett.3c02758
ACS Energy Lett. 2024, 9, 547−555

(62) Zheng, W. iR Compensation for Electrocatalysis Studies: Considerations and Recommendations. *ACS Energy Lett.* **2023**, *8* (4), 1952−1958.
(63) Son, Y. J.; Marquez, R. A.; Kawashima, K.; Smith, L. A.; Chukwuneke, C. E.; Babauta, J.; Mullins, C. B. Navigating iR Compensation: Practical Considerations for Accurate Study of Oxygen Evolution Catalytic Electrodes. *ACS Energy Lett.* **2023**, *8* (10), 4323−4329.
(64) Marin, D. H.; Perryman, J. T.; Hubert, M. A.; Lindquist, G. A.; Chen, L.; Aleman, A. M.; Kamat, G. A.; Niemann, V. A.; Stevens, M. B.; Regmi, Y. N.; Boettcher, S. W.; Nielander, A. C.; Jaramillo, T. F. Hydrogen Production with Seawater-Resilient Bipolar Membrane Electrolyzers. *Joule* **2023**, *7*, 765.
(65) Arges, C. G.; Parrondo, J.; Johnson, G.; Nadhan, A.; Ramani, V. Assessing the Influence of Different Cation Chemistries on Ionic Conductivity and Alkaline Stability of Anion Exchange Membranes. *J. Mater. Chem.* **2012**, *22* (9), 3733−3744.
(66) Wang, L.; Rojas-Carbonell, S.; Hu, K.; Setzler, B. P.; Motz, A. R.; Ueckermann, M. E.; Yan, Y. Standard Operating Protocol for Ion-Exchange Capacity of Anion Exchange Membranes. *Front. Energy Res.* **2022**, *10*, 887893.

https://doi.org/10.1021/acsenergylett.3c02758
ACS Energy Lett. 2024, 9, 547−555